Stresses induced by a demolition agent in non-explosive rock fracturing

J. Shang[1], Z. Zhao[1], M. M. Aliyu[2]

[1]Nanyang Centre for Underground Space, School of Civil and Environmental Engineering, Nanyang Technological University, Singapore.

[2]Department of Civil Engineering Technology, Ramat Polytechnic, Maiduguri, Nigeria.

This is a PDF file of an unedited manuscript that has been accepted for publication. The manuscript will undergo copyediting, typesetting, and review of the resulting proof before it is published in its final form. Please note that during the production process errors may be discovered which could affect the content.

Please approach the final version via https://doi.org/10.1016/j.ijrmms.2018.04.049

Abstract

Stresses induced by a demolition agent in non-explosive rock fracturing was analysed using the theory of elasticity and the thick-walled cylinder principle. Circumferential and radial stresses in rock induced by an internally pressurized hole was first analysed under plane strain condition. Stresses perpendicular to the line connecting two adjacent holes were calculated based on coordinate transformation. A parametric study was carried out to investigate the influence of spacing and size of hole on the stress distribution. The analytical model provides a method to determine the optimum hole spacing and size as well as the time needed for fracturing rocks with properties similar to those employed to determine the pressure-time function of the demolition agent. It is found that tensile stress decreased dramatically with the increasing of hole spacing, while it increased with increment of hole size but the influence of spacing on stress changes was more significant than that of hole size. It is also concluded from the study that tensile stress in the middle of two holes decreased dramatically with a logarithmic distribution when solely increasing hole spacing. As can be anticipated more time is required for rock fracturing and breaking when hole spacing is increased for both soft and hard rocks.

Key works: Stress; Non-explosive rock fracturing; Rock engineering; Demolition agent; Analytical solution

1. Introduction

Non-explosive rock fracturing has been widely used in rock engineering projects such as quarry, mining, underground infrastructure construction and rock slope engineering. Fig. 1a shows a rock slope formed by a demolition agent (DA) at the Castle Peak Road in Hong Kong where blasting may pose a significant threat to human safety and was not allowed. An underground tunnel was excavated by a PRS-95 hydraulic splitter in the construction of the Mass Transit Railway (Admiralty section, Hong Kong) (see Fig. 1b). The major advantage of this "silent" rock fracturing method is no fly rock, no vibration and controllability.

Despite the significant growth in the use of the controlled rock fracturing method, more guidance for design of hole patterns in practical rock engineering would be helpful. Spacing and diameter of holes are often empirically determined for a certain lithology and requirement. Diameter of holes are generally recommended between 30 and 65 mm depending on rock property, with a spacing of holes generally ranging from 200 to 1000 mm[1].

An empirical model was developed based on dimensional and polynomial regression analysis to determine hole spacing[2]. Gómez and Mura[3] investigated the relationship between hole diameter (l) and hole spacing (d) and concluded that spacing is proportional to diameter which can be written as $d=kl$. In that study, the value of k was experimentally determined as: $k<8$ for hard rock, $8<k<12$ for medium hard rock and $12<k<18$ for soft rock.

Dowding and Labuz[4] reported that temperature and thermal sensitivity of rock material could influence hole spacing, and an optimum spacing of 8 times hole diameter was proposed. Natanzi et al.[5] experimentally investigated demolition of masonry walls using DA. An optimum hole pattern with a d/l of 57 and a spacing of 225 mm was reported. Actually, these studies ignored the influence of time on fracturing when investigating the relationship between spacing and diameter.

Knowledge of pressure from DA has a great importance for an improved understanding of rock fracturing. An experimental methodology to determine the internal pressure of a single hole under an expansive load has been reported by measuring the tangential strain on the external boundary of a pipe wall that was internally pressurized[6]. In that study, the pressure was suggested to be calculated taking into account three independent parameters including hole diameter, loading time and Young's modulus. The research however failed to consider the interactions of neighbouring holes under expansive loads, which is very common in practical rock engineering.

There have been some publications regarding the stresses around holes in an infinite plate. Ling[7] investigated the stresses in a plate containing two equal circular holes. The aim of that study was to introduce a theoretical solution of stresses along the edges of holes under external tension load. Haddon[8] studied the stresses around two unequal holes in an infinite plate using the conformal mapping and complex variable methods. Based upon the Love's stress function, Ling et al.[9] presented an analytical solution for the stresses in a thick plate containing a cavity with a zero surface stress. The aforementioned investigations succeeded in formulating analytical solutions for stresses around holes but none of these researches can be directly used to understand the stress distribution by DA when fracturing rock because of the time dependent nature of the expansive pressure. On the other hand, in the application of DA, stress concentration often occur around a hole[10; 11; 12] under incremental static loading in rock, which will lead to the initiation and coalescence of fracture between adjacent holes[13].

The aim of this paper is to investigate stresses between two neighbouring holes under incremental expansive pressure from DA. A mathematical model comprising two internally pressurized holes was developed and influential factors including hole layout, loading time and rock property were taken into account. The relationships between optimum hole spacing and size which can used as a guidance for design of hole patterns in practical rock engineering were respectively derived for hard and soft rocks.

2. Non-explosive demolition agent

The non-explosive DA in this paper refers to a commercially available chemical powder which can expand considerably on mixing with water. In rock engineering, circular holes are drilled and terminated within rock masses and these pre-drilled holes are then filled with a mixture of DA and water at the recommended ratio (3.3 Kg/L). The DA hardens gradually and expands to fracture rock, typically over 24 hours[15] . The interaction mechanism of two adjacent holes with DA is illustrated in Fig. 2. Tensile stress perpendicular to the line connecting the two holes is generated by compression (due to the expansion of the DA within the holes); and the rock material in between will be fractured when the tensile stress exceeds the tensile strength of the rock.

3. Mathematical model and analysis

3.1 Stresses around a single internally pressurized hole

In this paper, the stresses arising from the interaction of two neighbouring holes is focused. Fig. 3 shows two symmetrical holes internally pressurised and the stresses acting on an element arising from Hole 2 in a polar coordinate. Assuming the two symmetrical holes with an equal radius of r_i are drilled in an elastic-plastic rock media. The DA is injected into the pre-drilled holes. The pressure (*p*) generated from the DA acts on the inside wall of the holes. The problem could be simplified as the interaction of two thick-walled rock cylinders internally pressurised. For the assumed cylinder, the inner radius is r_i and the outer radius r_0 equals to the hole spacing (*d*, from centre).

The pre-drilled Hole 2 and the surrounding rock material can be treated like a pressurised cylinder (Fig.3), and this problem can be simplified to plane strain state assuming the hole depth is infinite. In polar coordinates, the general stress equations of equilibrium without body force based on theory of elasticity can be given as[16]:

$$\begin{aligned}
&\frac{\partial \sigma_r}{\partial r}+\frac{1}{r}\frac{\partial \tau_{r\theta}}{\partial \theta}+\frac{\partial \tau_{r0}}{\partial 0}+\frac{\sigma_r-\sigma_\theta}{r}=0\\
&\frac{\partial \tau_{\theta r}}{\partial r}+\frac{1}{r}\frac{\partial \tau_{\theta}}{\partial \theta}+\frac{\partial \tau_{\theta 0}}{\partial 0}+2\frac{\tau_{\theta r}}{r}=0\\
&\frac{\partial \tau_{0r}}{\partial r}+\frac{1}{r}\frac{\partial \tau_{0\theta}}{\partial \theta}+\frac{\partial \sigma_{0}}{\partial 0}+\frac{\tau_{0r}}{r}=0
\end{aligned} \tag{1}$$

where *r* is the radius and θ is the azimuth in polar coordinates; the direction of σ_0 is perpendicular to the yz plane.

In the plane strain situation, the expand of hole surface is free, thus:

$$\sigma_0=0 \tag{2}$$

The general equations can be rewritten as:

$$\begin{aligned}
&\frac{\partial \sigma_r}{\partial r}+\frac{1}{r}\frac{\partial \tau_{r\theta}}{\partial \theta}+\frac{\partial \tau_{r0}}{\partial 0}+\frac{\sigma_r-\sigma_\theta}{r}=0\\
&\frac{\partial \tau_{\theta r}}{\partial r}+\frac{1}{r}\frac{\partial \tau_{\theta}}{\partial \theta}+\frac{\partial \tau_{\theta 0}}{\partial 0}+2\frac{\tau_{\theta r}}{r}=0\\
&\frac{\partial \tau_{0r}}{\partial r}+\frac{1}{r}\frac{\partial \tau_{0\theta}}{\partial \theta}+\frac{\tau_{0r}}{r}=0
\end{aligned} \tag{3}$$

This problem is symmetrical about *y*-axis as well as the line in the middle which is perpendicular to the line connecting the two holes, thus $\frac{\partial}{\partial\theta}=0$. Also, the radial deformation is uniform ($\tau_{r\theta}=\tau_{\theta 0}=\tau_{r0}=0$). Thus, Eq. (3) reduces to:

$$\frac{\partial\sigma_r}{\partial r}+\frac{\sigma_r-\sigma_\theta}{r}=0 \tag{4}$$

A standard solution for Eq. (4) is:

$$\sigma_r=\mathrm{c}\,r^{\mathrm{n}} \tag{5}$$

where c and n are constants.

The boundary conditions for a thick-walled cylinder with only internal pressure is:

$$\begin{cases}\sigma_r=-p\ (r=r_i)\\ \sigma_r=0 \qquad (r=r_0=d)\end{cases} \tag{6}$$

Substituting Eq. (6) into Eq. (5), The radial and circumferential stresses can be expressed as:

$$\begin{aligned}\sigma_r&=\frac{r_i^2 p(1-\frac{d^2}{r})}{d^2-r_i^2}\\ \sigma_\theta&=\frac{r_i^2 p(1+\frac{d^2}{r})}{d^2-r_i^2}\end{aligned} \tag{7}$$

3.2 Principal stresses perpendicular to the line connecting the two adjacent holes

To obtain the principal stresses on each element, the stresses in polar coordinates were transformed to Cartesian coordinates. Assuming the y-axis direction along the line connecting the two adjacent holes, and z-axis direction normal to the line, as shown in Fig. 3. The equations transforming from polar to Cartesian coordinates can be written as:

$$\begin{aligned}\sigma_{yy}&=\sigma_r\cos_\theta^2+\sigma_\theta\sin_\theta^2\\ \sigma_{zz}&=\sigma_r\sin_\theta^2+\sigma_\theta\cos_\theta^2\end{aligned} \tag{8}$$

where σ_{yy} is the principal stress along the line connecting the two pre-drilled holes in Cartesian coordinate system, and σ_{zz} is the principal stress perpendicular to the line. Note that if σ_{yy} and σ_{zz} work out to be positive, it is tension and if it is negative, it is compression.

From Eqs. (7) and (8), the principal stresses at any positions perpendicular to the line connecting the two adjacent holes can be written as:

$$\begin{aligned}\sigma_{zz} &= \frac{r_i^2 p}{d^2-r_i^2}\left(\sin^2\theta_1 - \frac{d^2}{r_1^2}\sin^2\theta_1 + \cos^2\theta_1 + \frac{d^2}{r_1^2}\cos^2\theta_1 + \sin^2\theta_2 - \frac{d^2}{r_2^2}\sin^2\theta_2 + \cos^2\theta_2 + \frac{d^2}{r_2^2}\cos^2\theta_2\right)\\ &= \frac{r_i^2 p}{d^2-r_i^2}\left[2 + \frac{d^2}{r_1^2}(\cos^2\theta_1 - \sin^2\theta_1) + \frac{d^2}{r_2^2}(\cos^2\theta_2 - \sin^2\theta_2)\right]\\ &= \frac{r_i^2 p}{d^2-r_i^2}\left[2 + d^2\left(\frac{1-2\sin^2\theta_1}{r_1^2} + \frac{1-2\sin^2\theta_2}{r_2^2}\right)\right]\end{aligned} \quad (9)$$

where r_1 and r_2 are the distance from any positions to the centres of Hole 1 and Hole 2, respectively. θ_1 and θ_2 are illustrated in Fig 3.

It is known that the pressure arising from DA is nonlinearly related with hole radius, time and mode-I fracture toughness of rock[2; 6], which can be defined as:

$$p = f(r_i, t, K_{IC}) = 0.12\, r_i^{0.407}\, t^{0.938}\, (37 K_{IC} - 1.6)^{0.493} \qquad 0 \le t \quad (10)$$

where r_i is the radius of the hole (m), t is the loading time (h) and K_{IC} denotes mode-I fracture toughness (MPa·m$^{1/2}$).

It is worthwhile emphasizing that, in Eq. (10), only three parameters (i.e., loading time, hole size and rock strength property) are considered, due to the fact that these three parameters dominantly affect the pressure from DA[6; 14; 17]. For example, rock strength affects the expansive pressure from DA. Because the increase of Young' modulus or fracture toughness of rock will lead to an increase of confinement to the expansion/hydration of DA, for which the DA can generate a high pressure[2; 17].

It has been reported that temperature contributes the hydration process of DA, thereby higher expansive pressure can be generated at higher temperatures[4; 17; 18]. However, a quantitative relation/equation between temperature and the performance of DA (in terms of expansive pressure) is still not available, as such further work needs to be performed in this regard to further improve the prediction performance of Eq. (10).

Substituting Eq. (10) into Eq. (9), the principal stresses along z-axis can be rewritten as:

$$\sigma_{zz} = \frac{r_i^2 * f(r_i, t, K_{IC})}{d^2 - r_i^2}\left[2 + d^2\left(\frac{1-2\sin^2\theta_1}{r_1^2} + \frac{1-2\sin^2\theta_2}{r_2^2}\right)\right]$$
$$= \frac{0.12\, r_i^{2.407} * t^{0.933}(37K_{IC} + 41.6)^{0.493}}{d^2 - r_i^2}\left[2 + d^2\left(\frac{1-2\sin^2\theta_1}{r_1^2} + \frac{1-2\sin^2\theta_2}{r_2^2}\right)\right] \quad (11)$$

4 Parametric study and discussion

For a certain rock and working environment, spacing and size of holes are key parameters to be considered by a practitioner to maintain an optimum use of DA. To understand the influence of these two parameters on principal tensile stresses, a parametric study was carried out. Midgley Grit sandstone (MGS) and Horton Formation siltstone (HFS), which respectively represent soft and hard rocks were employed in the parametric study. The uniaxial tensile strengths of MGS and HFS are 2.1 and 12.1, respectively; and the mode-I fracture toughness of these two rocks are 0.49 and 1.56, respectively[19].

4.1 Influence of hole spacing

Fig. 4 shows the principal tensile stress against the hole spacing for fracturing MGS (soft rock). Spacing of holes was analysed at various values from 20 to 2000 mm with an equal interval of 50 mm. For each situation, the loading time (*t*) was considered at 1, 2, 3, 5, 10, 15, 20, and 25 h, respectively, assuming that the DA can work up to 25 hours[14].

Note that for the sake of simplification, the principal tensile stress shown in Fig. 4 represents the stress at the middle of the two holes, thus:

$$r_1 = r_2 = d/2 \quad (12)$$

$$\theta_1 = \theta_2 = 0 \quad (13)$$

Eq. (11) is simplified as:

$$\sigma_{zz} = \frac{10 r_i^2 p}{d^2 - r_i^2} = 1.2\frac{t^{0.933} \cdot r_i^{2.407}(37K_{IC} + 41.6)^{0.493}}{d^2 - r_i^2} \quad (14)$$

As shown in Fig. 4, the principal tensile stress decreased significantly when the hole spacing was increased. The rock will be fractured when the principal tensile stress equals to the tensile strength of MGS (indicated by the horizontal dashed lines in Fig. 4). The time needed for fracturing MGS depends on hole spacing for a certain hole size. For example, for the hole with a radius of 27 mm (Fig. 4a), it took 20 hours for fracturing MGS when the hole spacing was 0.23 m, while it rose to 25 hours when the spacing was increased up to 0.26 m. The influence of the hole spacing on fracturing time became much larger at a specific hole radius of 100 mm. As can be seen in Fig. 4e, it required just 1 hour for fracturing MGS with a hole spacing of 0.29 m but 25 hours when the hole spacing reached up to 1.21 m.

Fig. 5 shows the relationship between the stress and spacing of hole for fracturing HFS (brittle hard rock). As can be seen, it allowed a slightly higher value of hole spacing for HFS compared with MGS at the same hole radius. For example, the spacing was 1.21 m for fracturing MGS at a certain hole radius of 100 mm (Fig. 4e); while it can be increased to 1.32 m for fracturing HFS under the same hole radius (Fig. 5e). The increase in spacing is due to the increment of expansive pressure from DA as a result of the increase of rock strength. In other words, hard brittle rock like HFS can provide more confinement during the hydration of DA, leading to the increment of expansive pressure from DA. Whereas the interaction between DA and MGS became weaker due to the comparatively lower confinement that can be provided by the soft rock, thus resulting in a lower expansive pressure from DA.

As shown in Figs. 4 and 5, the optimum hole spacing can be determined for a given hole size and an expected loading time (which can be determined based on project schedule). For example, the optimum hole spacing for fracturing HFS is around 1.0 m when the hole radius is 80 mm and the loading time is 25 hours (Fig. 5d). For this case, selection of a smaller hole spacing (e.g., <1.0 m) will lead to an excessive use of DA (because more holes need to be drilled), which will evidently increase project budget. The optimum hole spacing against the time needed for fracturing both soft and hard rocks (at some certain hole sizes) was plotted in Fig. 6 and polynomial curves are fitted. It can be seen that the optimum hole spacing is increased when the loading time is increased for both soft and hard rocks as well as different hole sizes. Also as mentioned earlier, for a certain hole size and a specific loading time, the optimum hole spacing can be slightly larger for fracturing hard rock than that for fracturing soft rock.

4.2 Influence of hole size

In this section, the influence of hole size on stress was investigated, while hole spacing remained constant. Figs. 7 and 8 show the principal tensile stress against hole radius for fracturing MGS and HFS, respectively. As observed, the stress increased significantly when the hole radius increases for both soft and hard rocks, which means that more DA will be used for fracturing the rocks. It was also observed that the influence of spacing increment on stress (leading to a stress decrement) is more significant than that from hole size increment (leading to stress increment). For example, it took 1 hour for fracturing HFS when the hole radius was 70 mm and spacing was 200 mm (Fig. 8a), while the time needed soared to at least 20 hours when both hole radius and spacing were increased (up to 86 and 1000 mm repressively, see Fig. 8e).

Fig. 9 shows the relationship between the optimum hole radius and the time needed for fracturing soft and hard rocks. It can be seen that the time required for fracturing both soft and hard rocks decreased with the increment of the hole radius (for a specific hole spacing). For example, as shown in Fig. 9a, it took 1 hour for fracturing MGS when holes with a radius of 74 mm and a spacing of 200 mm were used. While the loading time rose up to 25 hours when the hole radius dropped to 22 mm with a same spacing. Similar situation occurred for the hard rock.

Based on the above analysis, the optimum hole spacing was plotted against hole radius considering rock strength, as shown in Fig. 10. For a certain rock engineering project, it is suggested that hole size can be confirmed first based on the available drilling apparatus, and then the optimum hole spacing can be evaluated based on the results of this study.

5 Conclusion

In this paper, an analytical model was presented to investigate the stresses arising from a non-explosive demolition agent when fracturing rock based on the elastic theory and thick-walled cylinder principle. The analytical model provides a method to determine the optimum hole spacing and size as well as the time needed for fracturing rocks with properties similar to those employed to determine the pressure-time function of the demolition agent. The influences of hole size and spacing on principal stress were examined taking into account loading time and lithology. Several conclusions can be drawn from this study: (1) Tensile stress decreased dramatically with the increasing of hole spacing, while it increased with increment of hole size but the influence of spacing on stress changes was more significant than that of hole size; (2) For a certain rock engineering project, the optimum spacing can be determined when hole size is constrained by drilling rigs; and the time needed for fracturing rock can be estimated based on the results of this study; and (3) the potential influence of temperature on the performance of demolition agent was not considered in the study, which needs to be addressed in future research.

Results from this study can provide a scientific guidance in terms of layout design and time management when using demolition agent for fracturing rock. Additionally, the implementation of numerical analysis for investigating non-explosive rock fracturing can probably be achieved based on the stress analysis results presented in the study.

Reference

1. Huynh MP, Laefer, DF. Expansive cements and soundless chemical demolition agents: state of technology review. In: 11th Conference on Science and Technology, Ho Chi Minh City Vietnam, 21-23 October 2009: 209-214.

2. Arshadnejad S, Goshtasbi K, Aghazadeh J. A model to determine hole spacing in the rock fracture process by non-explosive expansion material. Int J Min Met Mater. 2011; 18(5):509-514.

3. Gómez C, Mura T. Stresses caused by expansive cement in borehole. J Eng Mech. 1984; 110(6):1001-1005.

4. Dowding CH, Labuz JF. Fracturing of rock with expansive cement. J Geotech Eng. 1982; 108(10):1288-1299.

5. Natanzi AS, Laefer DF, Mullane S. Chemical demolition of unit masonry: a preparatory study. In: 10th International Conference on Structural Analysis of Historical Constructions: Anamneris, Diagnosis, Therapy, Controls (SAHC2016), Leuven, Belgium, 13-15 September: 1-13.

6. Gholinejad M, Arshadnejad S. An experimental approach to determine the hole-pressure under expansion load. J South Afr Inst Min Metail. 2012; 112:631-635.

7. Ling CB. On the stresses in a plate containing two circular holes. J Appl Phys. 1948; 19(77):77-81.

8. Haddon AW. Stresses in an infinite plate with two unequal circular holes. Q J Mech Appl Math. 1967; 20: 277-291.

9. Ling CB, Va B, Tsai CP. Stress in a thick plate containing an eccentric spherical inclusion or cavity. Acta Mech. 1969; 7:169-186.

10. Coates DF, Yu YS. A note on the stress concentrations at the end of a cylindrical hole. Int J Rock Mech Min Sci. 1970; 7:583-588.

11. Zimmerman RW. Stress concentration around a pair of circular holes in a hydrostatically stressed elastic sheet. J Appl Mech. 1988; 55(2):487-488.

12. Li Y, Peng J, Zhang F, Qiu Z. Cracking behavior and mechanism of sandstone containing a pre-cut hole under combined static and dynamic loading. Eng Geol. 2016; 213:64-73.

13. Arshadnejad S, Niu J. Birth of the first crack and its growth under incremental static loading between two holes in brittle rocks. J Earth Eng. 2014; 1(1):1-15.

14. Shang J, West LJ, Hencher SR, Zhao Z. Tensile strength of large-scale incipient rock joints: A laboratory investigation. Acta Geotech. 2017; https://doi.org/10.1007/s11440-017-0620-7

15. Shang J, Hencher SR, West LJ, Handley K. Forensic excavation of rock masses: A technique to investigate discontinuity persistence. Rock Mech Rock Eng. 2017; 50(11):2911-2928.

16. Murakami Y. Theory of elasticity and stress concentration, Wiley, West Sussex. 2016: pp. 445.

17. Jin ZZ, Liao H, Zhu W. Splitting mechanism of rock and concrete under expansive pressure. In: Proceedings of Demolition and Reuse of Concrete and Masonry, Japan. 1988: pp 141.

18. Hinze H, Brown J. Properties of soundless chemical demolition agents. J. Constr. Eng. Manage. 1994; 120(4):816-827.

19. Shang J. Persistence and tensile strength of incipient rock discontinuities. PhD thesis, the University of Leeds, United Kingdom. 2016: pp 248.

Figure captions

Fig 1 a A demolition agent used to form slopes at the Castle Peak Road in Hong Kong where blasting was not allowed. Hammer for scale; **b** A hydraulic splitter (model PRS-95) was employed for the non-explosive fracturing of rock in construction of the Mass Transit Railway (Admiralty section) in Hong Kong.

Fig 2 Interaction mechanism of two neighbouring holes subjected to the expansive pressure from a non-explosive demolition agent. Redrawn from Natanzi et al.[5]

Fig 3 Model of two symmetrical holes internally pressurized. Stresses acting on an element solely arising from Hole 2 is presented in polar coordinate. r is the radius and θ is the azimuth in polar coordinate.

Fig 4 Principal tensile stress against hole spacing for Midgley Grit sandstone (soft rock).

Fig 5 Principal tensile stress against hole spacing for Horton Formation siltstone (hard rock).

Fig 6 Relationships between the optimum hole spacing and the time required for fracturing soft rock (**a**) and hard rock (b).

Fig 7 Principal tensile stress against hole size for Midgley Grit sandstone (soft rock).

Fig 8 Principal tensile stress against hole size for Horton Formation siltstone (hard rock).

Fig 9 Relationships between the optimum hole size and the time required for fracturing soft rock (**a**) and hard rock (b).

Fig 10 Relationships between optimum hole size and hole spacing for fracturing both soft and hard rocks.

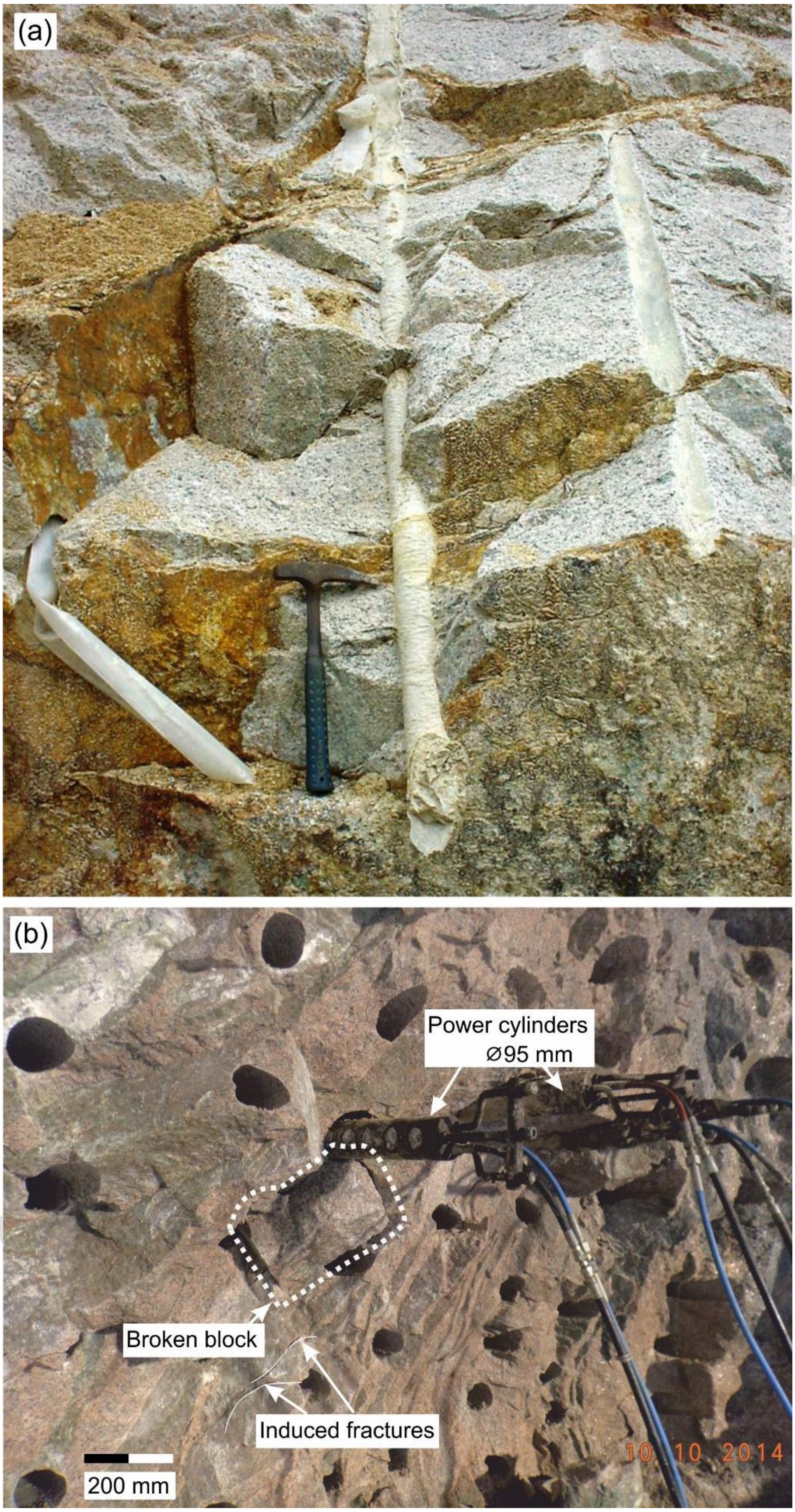
(a)
(b)
Power cylinders
Ø95 mm
Broken block
Induced fractures
200 mm
10 10 2014

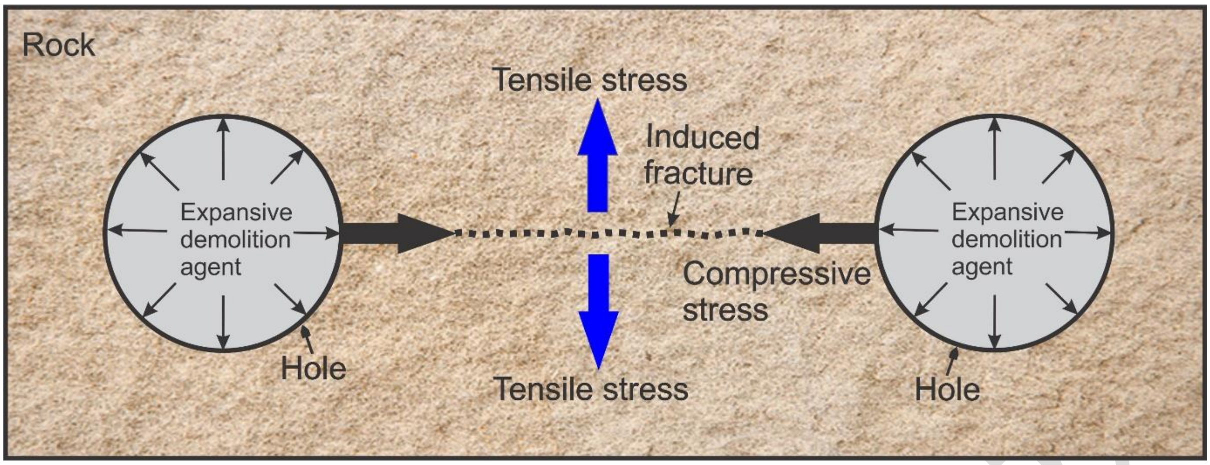
Rock
Tensile stress
Induced
fracture
Expansive
demolition
agent
Expansive
demolition
agent
Compressive
stress
Hole
Tensile stress
Hole

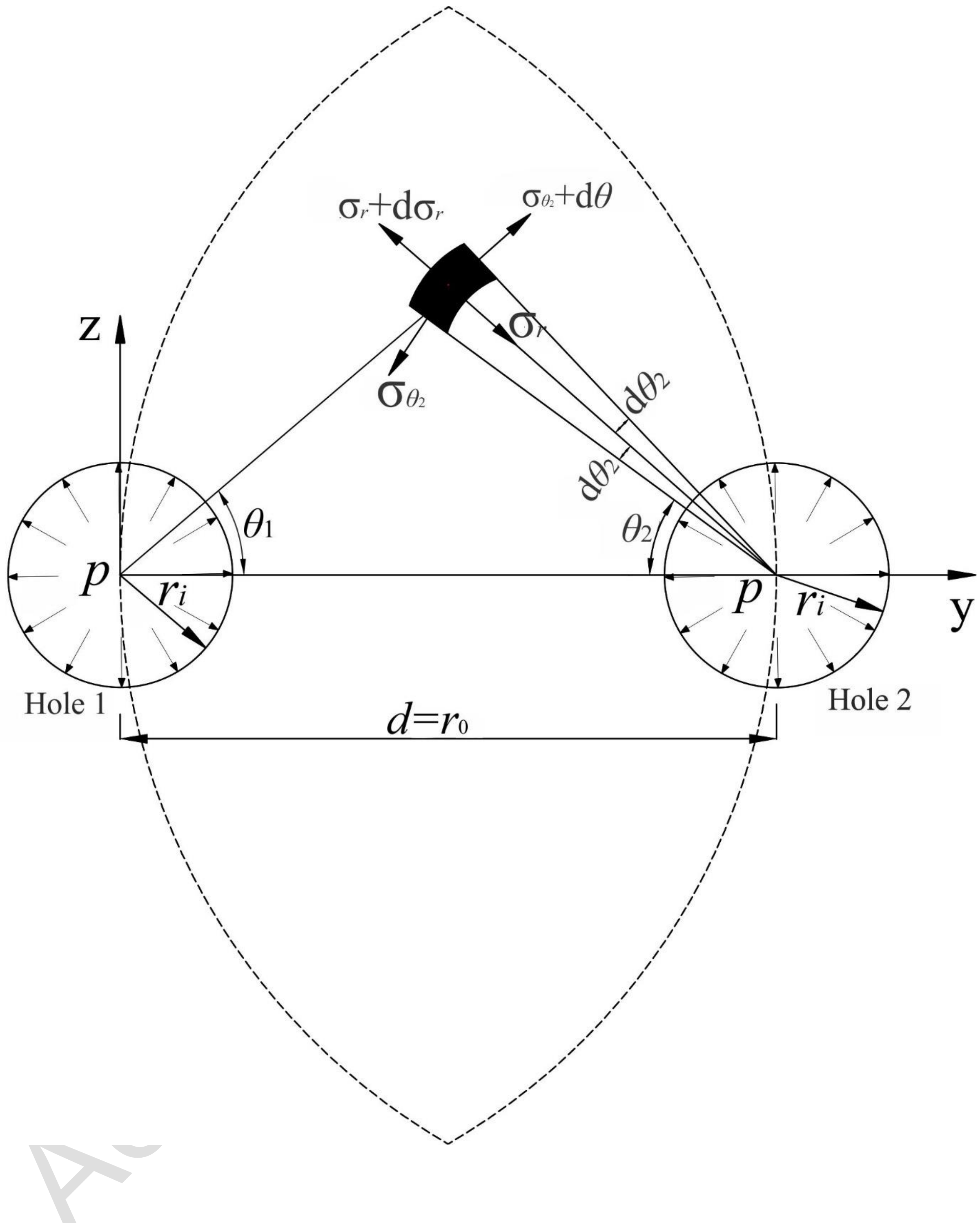

352

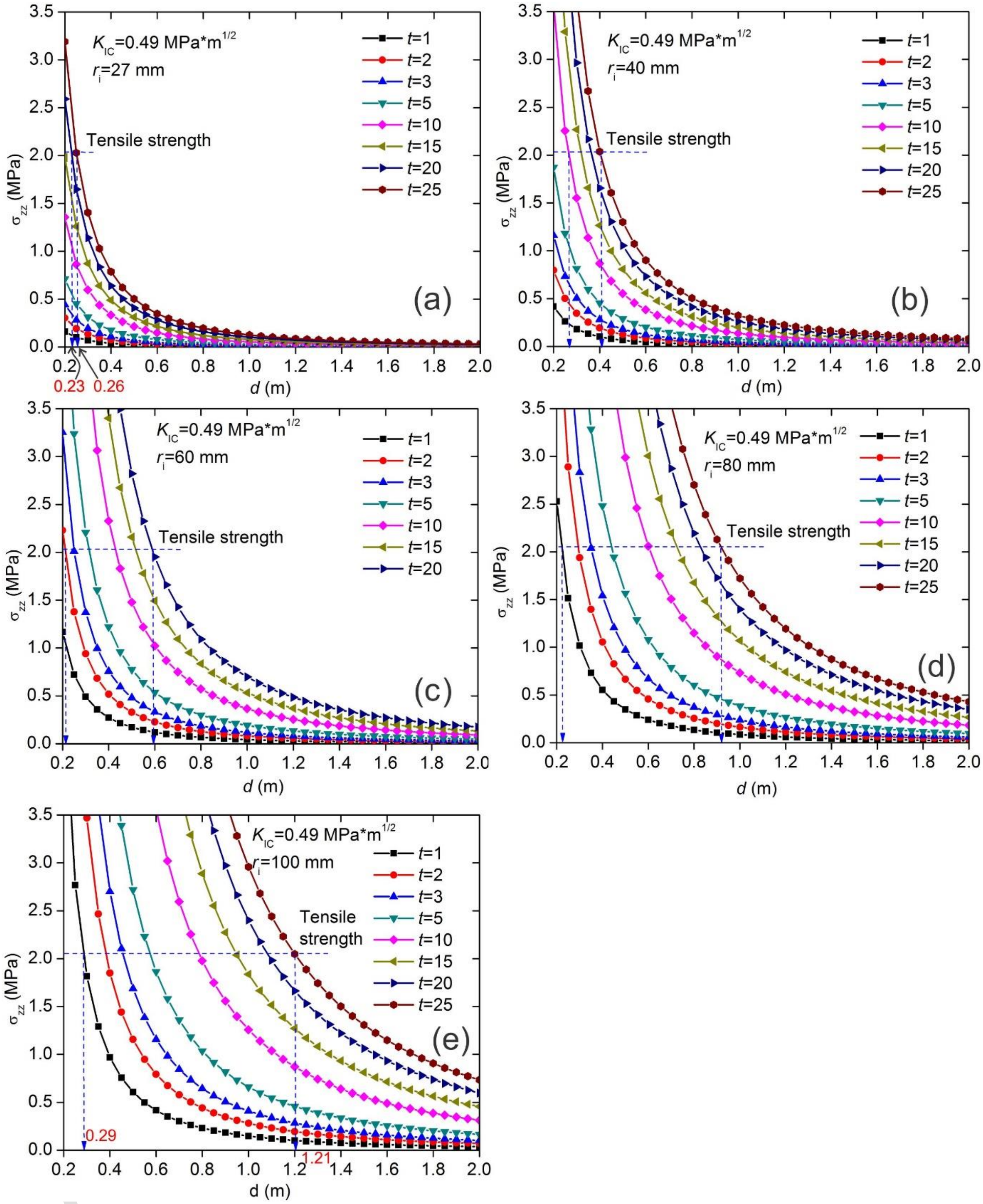

K_IC=0.49 MPa*m^1/2
r_i=27 mm
Tensile strength
(a)
0.23
0.26
r_i=40 mm
(b)
r_i=60 mm
(c)
r_i=80 mm
(d)
r_i=100 mm
(e)
0.29
1.21
t=1
t=2
t=3
t=5
t=10
t=15
t=20
t=25
σ_zz (MPa)
d (m)

353

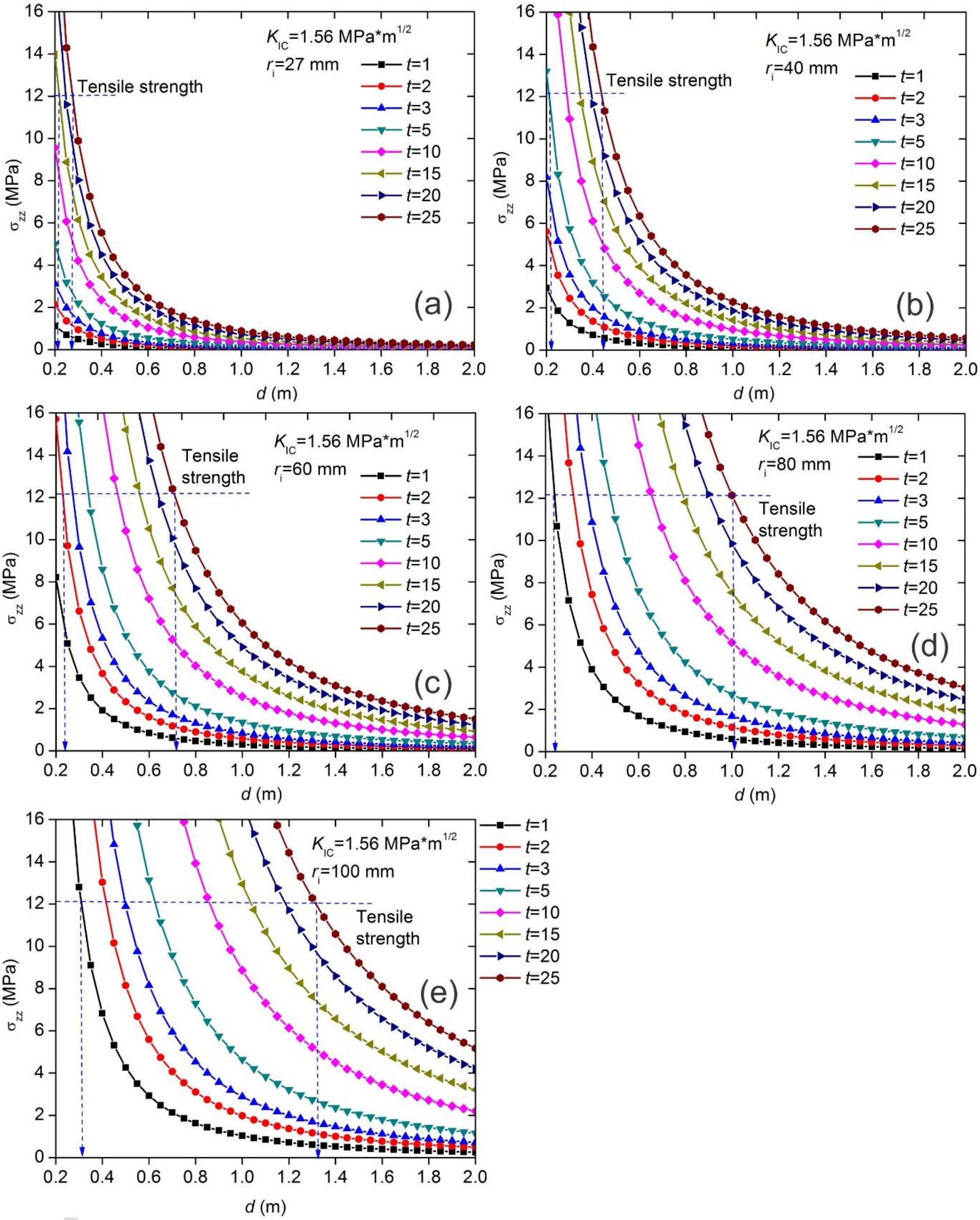
(a)
K_{IC}=1.56 MPa*m$^{1/2}$
r_i=27 mm
Tensile strength
(b)
K_{IC}=1.56 MPa*m$^{1/2}$
r_i=40 mm
Tensile strength
(c)
K_{IC}=1.56 MPa*m$^{1/2}$
r_i=60 mm
Tensile strength
(d)
K_{IC}=1.56 MPa*m$^{1/2}$
r_i=80 mm
Tensile strength
(e)
K_{IC}=1.56 MPa*m$^{1/2}$
r_i=100 mm
Tensile strength
t=1
t=2
t=3
t=5
t=10
t=15
t=20
t=25
σ_{zz} (MPa)
d (m)

354

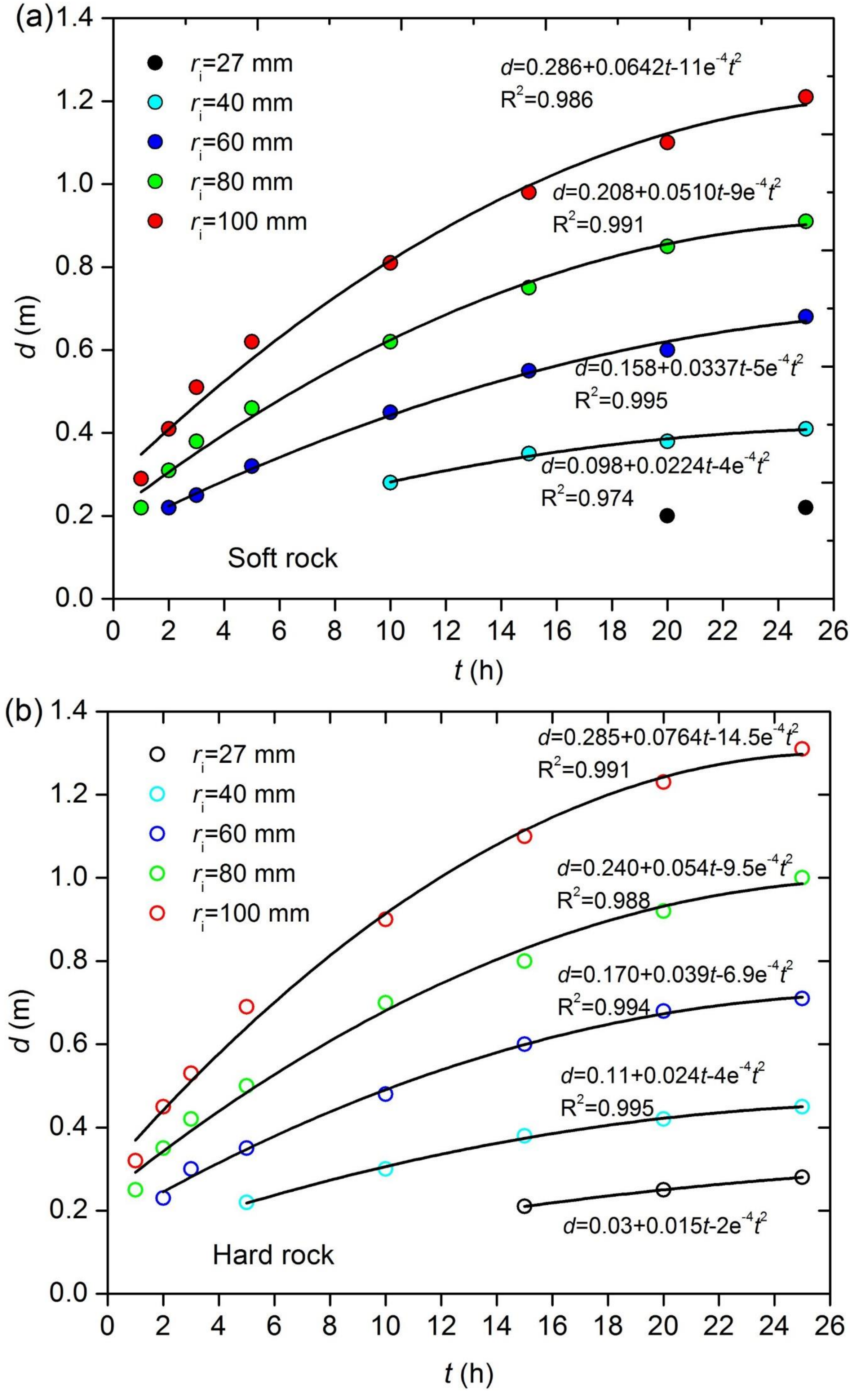
(a)
Soft rock
r_i=27 mm
r_i=40 mm
r_i=60 mm
r_i=80 mm
r_i=100 mm
d=0.286+0.0642t-11e$^{-4}t^2$
R^2=0.986
d=0.208+0.0510t-9e$^{-4}t^2$
R^2=0.991
d=0.158+0.0337t-5e$^{-4}t^2$
R^2=0.995
d=0.098+0.0224t-4e$^{-4}t^2$
R^2=0.974
d (m)
t (h)
(b)
Hard rock
r_i=27 mm
r_i=40 mm
r_i=60 mm
r_i=80 mm
r_i=100 mm
d=0.285+0.0764t-14.5e$^{-4}t^2$
R^2=0.991
d=0.240+0.054t-9.5e$^{-4}t^2$
R^2=0.988
d=0.170+0.039t-6.9e$^{-4}t^2$
R^2=0.994
d=0.11+0.024t-4e$^{-4}t^2$
R^2=0.995
d=0.03+0.015t-2e$^{-4}t^2$
d (m)
t (h)

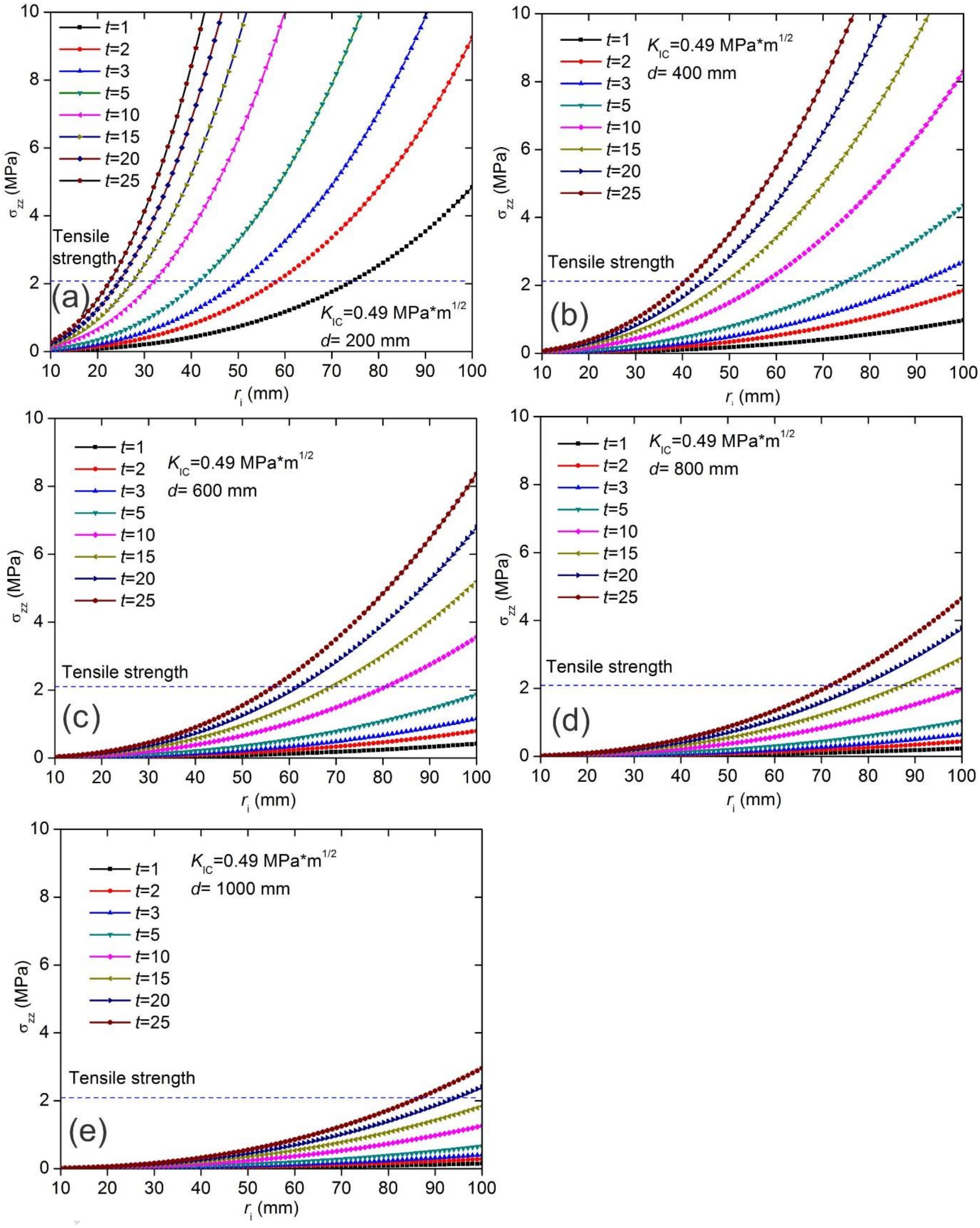

(a)
t=1
t=2
t=3
t=5
t=10
t=15
t=20
t=25
Tensile strength
K_IC=0.49 MPa*m^1/2
d= 200 mm
σ_zz (MPa)
r_i (mm)
(b)
K_IC=0.49 MPa*m^1/2
d= 400 mm
Tensile strength
(c)
K_IC=0.49 MPa*m^1/2
d= 600 mm
Tensile strength
(d)
K_IC=0.49 MPa*m^1/2
d= 800 mm
Tensile strength
(e)
K_IC=0.49 MPa*m^1/2
d= 1000 mm
Tensile strength

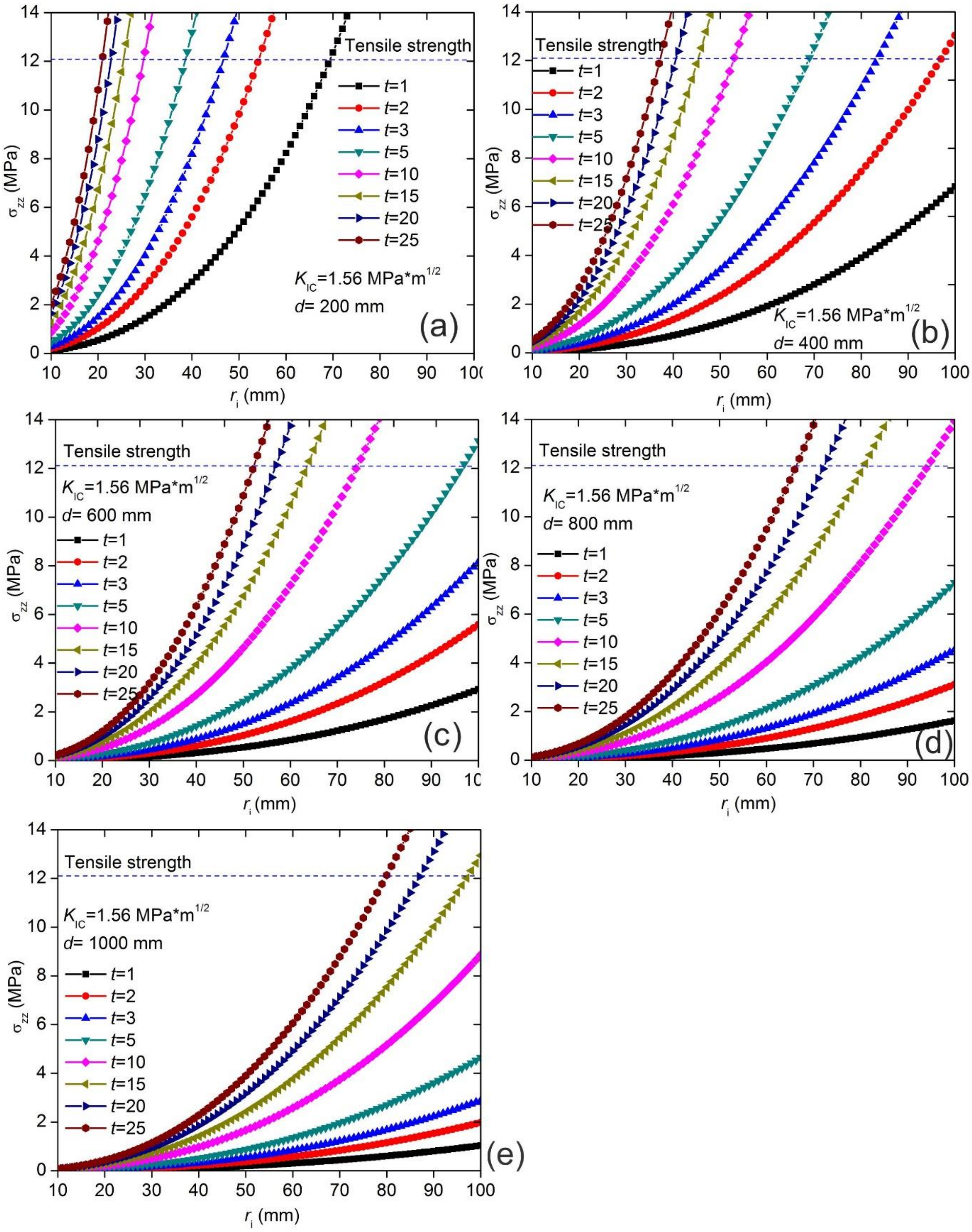

Tensile strength
t=1
t=2
t=3
t=5
t=10
t=15
t=20
t=25
K_IC=1.56 MPa*m^1/2
d= 200 mm
(a)
d= 400 mm
(b)
d= 600 mm
(c)
d= 800 mm
(d)
d= 1000 mm
(e)
σ_zz (MPa)
r_i (mm)

357

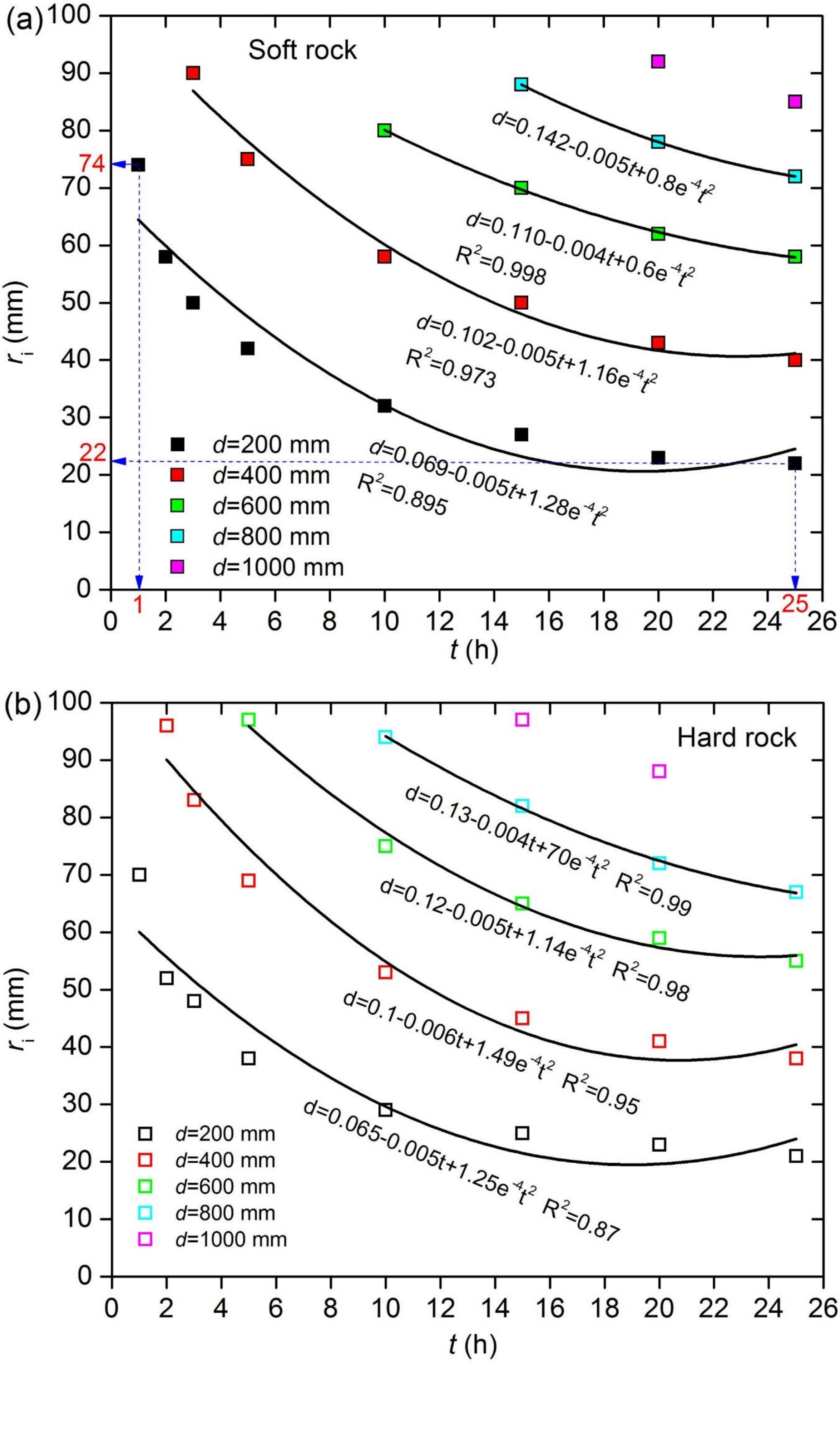
(a)
Soft rock
r_i (mm)
t (h)
74
22
1
25
d=0.142-0.005t+0.8e-4t2
d=0.110-0.004t+0.6e-4t2
R2=0.998
d=0.102-0.005t+1.16e-4t2
R2=0.973
d=0.069-0.005t+1.28e-4t2
R2=0.895
d=200 mm
d=400 mm
d=600 mm
d=800 mm
d=1000 mm
(b)
Hard rock
r_i (mm)
t (h)
d=0.13-0.004t+70e-4t2 R2=0.99
d=0.12-0.005t+1.14e-4t2 R2=0.98
d=0.1-0.006t+1.49e-4t2 R2=0.95
d=0.065-0.005t+1.25e-4t2 R2=0.87
d=200 mm
d=400 mm
d=600 mm
d=800 mm
d=1000 mm

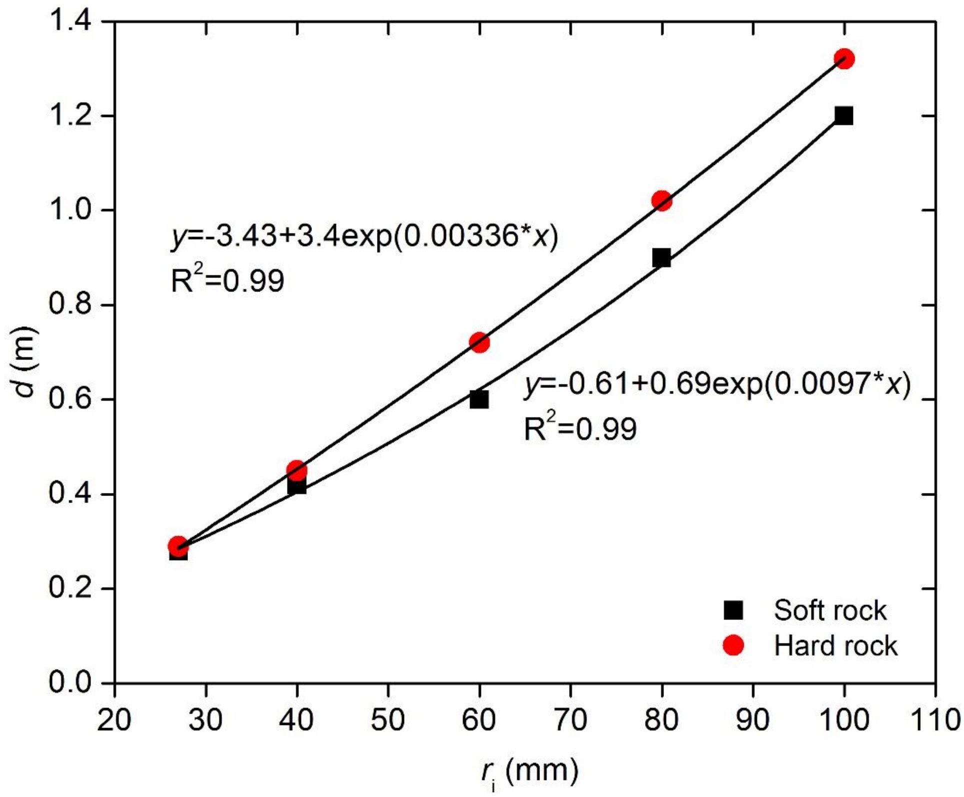
1.4
1.2
1.0
0.8
0.6
0.4
0.2
0.0
d (m)
y=-3.43+3.4exp(0.00336*x)
R2=0.99
y=-0.61+0.69exp(0.0097*x)
R2=0.99
Soft rock
Hard rock
20
30
40
50
60
70
80
90
100
110
ri (mm)

359